

GW150914: FIRST SEARCH FOR THE ELECTROMAGNETIC COUNTERPART OF A GRAVITATIONAL-WAVE EVENT BY THE TOROS COLLABORATION

MARIO C. DÍAZ^{*1}, MARTÍN BEROIZ^{1,2}, TANIA PEÑUELA^{1,3}, LUCAS M. MACRI⁴, RYAN J. OELKERS^{4,10}, WENLONG YUAN⁴, DIEGO GARCÍA LAMBAS⁵, JUAN CABRAL⁵, CARLOS COLAZO^{5, 6}, MARIANO DOMÍNGUEZ⁵, BRUNO SÁNCHEZ⁵, SEBASTIÁN GUROVICH⁵, MARCELO LARES⁵, MATÍAS SCHNEITER⁵, DARÍO GRAÑA⁵, VÍCTOR RENZI⁵, HORACIO RODRIGUEZ⁵, MANUEL STARCK⁵, RUBÉN VRECH⁵, RODOLFO ARTOLA⁵, ANTONIO CHIAVASSA FERREYRA⁵, CARLA GIRARDINI⁵, CECILIA QUIÑONES⁵, LUIS TAPIA⁵, MARINA TORNATORE⁵, JENNIFER L. MARSHALL⁴, DARREN L. DEPOY⁴, MARICA BRANCHESI⁷, ENZO BROCATO⁸, NELSON PADILLA⁹, NICOLAS A. PEREYRA¹, SOMA MUKHERJEE¹, MATTHEW BENACQUISTA¹ & JOEY KEY¹

Draft version September 18, 2018

ABSTRACT

We present the results of the optical follow-up conducted by the TOROS collaboration of the first gravitational-wave event GW150914. We conducted unfiltered CCD observations (0.35 – 1 μ m) with the 1.5-m telescope at Bosque Alegre starting \sim 2.5 days after the alarm. Given our limited field of view (\sim 100 \square'), we targeted 14 nearby galaxies that were observable from the site and were located within the area of higher localization probability.

We analyzed the observations using two independent implementations of difference-imaging algorithms, followed by a Random-Forest-based algorithm to discriminate between real and bogus transients. We did not find any *bona fide* transient event in the surveyed area down to a 5σ limiting magnitude of $r = 21.7$ mag (AB). Our result is consistent with the LIGO detection of a binary black hole merger, for which no electromagnetic counterparts are expected, and with the expected rates of other astrophysical transients.

Subject headings: Gravitational Waves, General relativity, GW150914, techniques: image processing

1. INTRODUCTION

The network of advanced ground-based gravitational wave (GW) interferometers constituted by the LIGO observatories (LIGO Scientific Collaboration et al. 2015), which started operations in September 2015 and by the VIRGO observatory (Acernese et al. 2015), which will join before the end of 2016, were designed to be capable of detecting GWs emitted by the mergers of neutron stars and/or black holes in binary systems out to distances of hundreds of Mpc (see Abbott et al. 2016b, and references therein). In anticipation of the operation of this network, on 2013 June 6 the LIGO-VIRGO collaboration (LVC) issued a worldwide call¹¹ to astronomers to participate in multi-messenger observations of astrophysical events recorded by the GW detectors, using a wide range of telescopes and instruments of “mainstream” astronomy.

Initially, triggers will be shared promptly only with astronomy partners who have signed a Memorandum of Understanding (MoU) with LVC involving an agreement on deliverables, publication policies, confidentiality, and reporting. It is expected that if the mergers of compact objects contain at least one neutron star, electromagnetic (EM) radiation will be emitted during the event. This EM counterpart, originating in the ejecta and its interaction with the surrounding environment could range from very short duration gamma-ray bursts to longer-duration emission at optical, near infrared (kilonova and short GRB afterglows) and radio wavelengths (e.g., Li & Paczyński 1998; Nakar & Piran 2011; Metzger & Berger 2012; Barnes & Kasen 2013; Berger 2014; Cowperthwaite & Berger 2015). Simultaneous detection of the event by GW and EM observatories could provide a more integrated astrophysical interpretation of the event and would be instrumental in producing better estimates for the distance and energy scales of the event.

Motivated to participate in these observations, we formed a collaboration named “Transient Optical Robotic Observatory of the South” (TOROS; Benacquista et al. 2014) which seeks to deploy a wide-field optical telescope on Cordón Macón in the Atacama Plateau of northwestern Argentina (Renzi et al. 2009; Tremblin et al. 2012). The collaboration planned to utilize other resources independently of the construction of this facility. On 2014 April 5, the TOROS collaboration signed a Memorandum of Understanding with LVC and participated during the first scientific run of the GW interferometers from September 2015 through January 2016. Two facilities were available to TOROS during this campaign: a Schmidt-Cassegrain 0.4-m telescope at Cordón Macón and a 1.5-m telescope at Estación Astrofísica Bosque Alegre (EABA) in Córdoba, Argentina.

* Corresponding author, mario.diaz@utrgv.edu

¹ Center for Gravitational Wave Astronomy, University of Texas Rio Grande Valley, Brownsville, TX, USA

² University of Texas at San Antonio, San Antonio, TX, USA

³ Ludwig Maximilian Universität Munich, Faculty of Physics, Munich, Germany

⁴ Mitchell Institute for Fundamental Physics & Astronomy, Department of Physics & Astronomy, Texas A&M University, College Station, TX, USA

⁵ Universidad Nacional de Córdoba, IATE, Córdoba, Argentina

⁶ Ministerio de Educación de la Provincia de Córdoba, Argentina

⁷ Università degli studi di Urbino, Urbino, Italy

⁸ INAF - Osservatorio Astronomico di Roma, Monte Porzio Catone, Italy

⁹ Instituto de Astrofísica, Pontificia Universidad Católica de Chile, Santiago, Chile

¹⁰ Current address: Physics & Astronomy Department, Vanderbilt University, Nashville, TN, USA

¹¹ <http://www.ligo.org/scientists/GWEMAlerts.php>

On 2015 September 14 at 09:50:45 UT, the two USA-based detectors of the Advanced LIGO interferometer network detected a high-significance candidate GW event designated GW150914 (Abbott et al. 2016a). This unexpected detection — observed four days before the first scientific run of the detectors was scheduled to start — constituted the first detection of the merger of a binary black hole (BBH) system and the first direct detection of gravitational waves. Due to the unexpected timing of the event, LVC provided spatial location information two days later, in the form of probability sky maps via a private GCN circular (Singer 2015, GCN#18330). TOROS was one of 25 teams that participated in the search for an electromagnetic counterpart in the southern hemisphere. We report here on the optical follow up of this event by the TOROS collaboration during 2015 September 16-17 using the 1.5-m EABA telescope (the smaller telescope at Macón was not operational at the time).

This paper is organized as follows: §2 discusses target selection and observations; §3 describes the data reduction, image differencing algorithms and the bogus/real classification; §4 presents our results and §5 summarizes our findings. Throughout this paper, we express magnitudes in the AB system and adopt a Λ CDM cosmology based on results from the Planck mission (Planck Collaboration et al. 2015).

2. OBSERVATIONS

For the first run of the LIGO detectors (O1) several low-latency analyses were prepared to receive and process signals from GWs. On 2015 September 16, the LIGO Virgo Collaboration (LVC) provided two all-sky localization probability maps for the event, based on them. Both the coherent Wave Burst (cWB; Klimenko et al. 2016) and the Omicron+LALInference Burst (oLIB; Lynch et al. 2015) search for un-modeled signals. The first one, a rapid localization analysis just searches for coherent power across both detectors while the second one, more refined, assumes a Sine-Gaussian content. The maps provided initial spatial localization of 50% and 90% confidence regions encompassing about 200 and 750 \square° , respectively (Singer 2015, GCN#18330).

We started our imaging campaign immediately after receiving the GCN circular and acquired the first epoch of observations on 2015 September 16 & 17. We obtained a second epoch of imaging (to serve as templates for the differencing pipelines) on 2015 December 5 & 6. We used an Apogee Alta U9 camera with a field of view (FoV) of $12'7 \times 8'5$ and an effective plate scale of $0''.75 \text{ pix}^{-1}$ after 3×3 binning. Since we wished to maximize our sensitivity, we conducted unfiltered (“white light”) observations spanning $0.35 < \lambda/\mu\text{m} < 1$. We obtained individual exposures of 60 s with a median seeing (FWHM) of $(2.8 \pm 0.6)''$. We typically obtained 10 images per field, reaching 5σ limiting magnitudes of $r = 21.7 \pm 0.3 \text{ mag}$ (see §3 for details).

The LIGO localization regions span several hundred square degrees (see Fig. 1) and vary depending on the algorithm. For instance, the 90% credible localization area for cWB covers to $310\square^\circ$ while others span up to $750\square^\circ$ (see table 1 in Abbott et al. 2016c). Regardless, all sky maps are consistent with a broad long arc in the Southern hemisphere and a smaller extension in the Northern hemisphere. The algorithm utilized for the CWB

estimations produces reasonably accurate maps for BBH signals, but underestimates the extent of high-confidence regions (Essick et al. 2015). As seen in Fig. 1, the adoption of maps from alternative algorithms (not available at the time our observations started) significantly reduces the fraction of the high-confidence region probed by our small FoV.

Previous work in the field (Nuttall & Sutton 2010; Abadie et al. 2012; Hanna et al. 2014) have shown that using a galaxy catalog can greatly increase the probability of finding an EM counterpart in the case of BNS or NSBH events. As the LIGO analysis was still ongoing at the time our observations had begun and the nature of the binary was unknown, we optimized the use of our small FoV by targeting nearby galaxies with the highest probability of hosting the event. The probabilities were based on the values of the pixel in the initial cWB map that contained the coordinates of a given galaxy. We used the Gravitational Wave Galaxy Catalog (GWGC; White et al. 2011), which is a compilation of catalogs homogenized into a list of ~ 53000 galaxies within 100 Mpc (with incompleteness starting at $D \sim 40$ Mpc). The GWGC provides reliable distances, blue magnitudes and other properties.

Table 1 lists the galaxies targeted in our search. They were selected using an in-house “scheduler” (a Python module of the TOROS pipeline). The scheduler set a list of criteria: (1) observability from our location ($30^\circ > \delta > -70^\circ$), (2) apparent magnitude $B \leq 21 \text{ mag}$, and (3) distance $D < 60 \text{ Mpc}$. We plan to add for future observations absolute magnitude $M_B \leq -21 \text{ mag}$ as an additional criterion. This cut in absolute magnitude is motivated by the expectation that in the nearby Universe the distribution of BNS and BHs should follow recent star formation due to the short merger timescales (see e.g. Phinney 1991; Belczynski et al. 2002). Once we cross-matched the LIGO sky maps with the filtered galaxies, we ranked the results by assigning individual probabilities $P_{g,i}$ (with i being the sky map pixel that contained the g -th galaxy). This enabled us to prioritize targets according to their location within the sky maps and their observability. Lastly, we ensured that all targets were mapped out to $\sim 5 \text{ kpc}$, which corresponds to the median offset distance of short GRBs from hosts galaxies measured from the optical afterglow observations (Church et al. 2011; Fong & Berger 2013; Berger 2014). This required tiling to cover the appropriate area for some targets. A total of 21 fields covering 14 galaxies were observed. These correspond to $\sim 4.4\%$ of the potential host galaxies listed in the GWGC that met selection criteria (2) & (3). We note that at $D \sim 60 \text{ Mpc}$, the GWGC is estimated to be complete at the $\sim 80\%$ level (White et al. 2011).

3. DATA ANALYSIS

The initial data reduction followed the standard steps of bias and dark subtraction, flat-fielding using twilight sky frames, and illumination correction, based on common routines available in PyRAF and independent Python modules that constitute the TOROS data processing pipeline. Astrometric solutions were derived using the *Astrometry* package (Lang 2009), a very robust algorithm based on *geometrical hashing* of asterisms and

TABLE 1
 TARGETED HOST GALAXIES

Date ¹	ID ²	RA	Dec.	t_{exp}	Tile #	D
		[deg]		[s]		[Mpc]
2015-09-16	IC1933	51.416101	-52.78547	600	1,2,3,4	17.45
2015-09-16	NGC1529	61.833301	-62.89993	600	5,6,7,8	54.76
2015-09-16	IC2038	62.225246	-55.99074	600	9,10,11,12	7.00
2015-09-16	IC2039	62.259901	-56.01172	600	9,10,11,12	7.63
2015-09-17	ESO058-018	102.593850	-71.03123	1020	13	52.23
2015-09-17	ESO084-015	65.550449	-63.61097	1140	14	14.99
2015-09-17	ESO119-005	72.072451	-60.29376	1080	15	9.73
2015-09-17	NGC1559	64.398901	-62.78358	900	16	12.59
2015-09-17	PGC016318	73.728898	-61.56747	1020	17	9.54
2015-09-17	PGC269445	100.209150	-71.33026	1140	18	54.83
2015-09-17	PGC280995	96.382499	-69.15257	1140	19	55.08
2015-09-17	PGC128075	64.859998	-60.53844	720	20	63.71
2015-09-17	PGC381152	63.584547	-58.20726	1200	21	13.26
2015-09-17	PGC075108	63.670349	-58.13199	1200	21	13.29

NOTE. — (1) local date of observation; (2) from White et al. (2011)

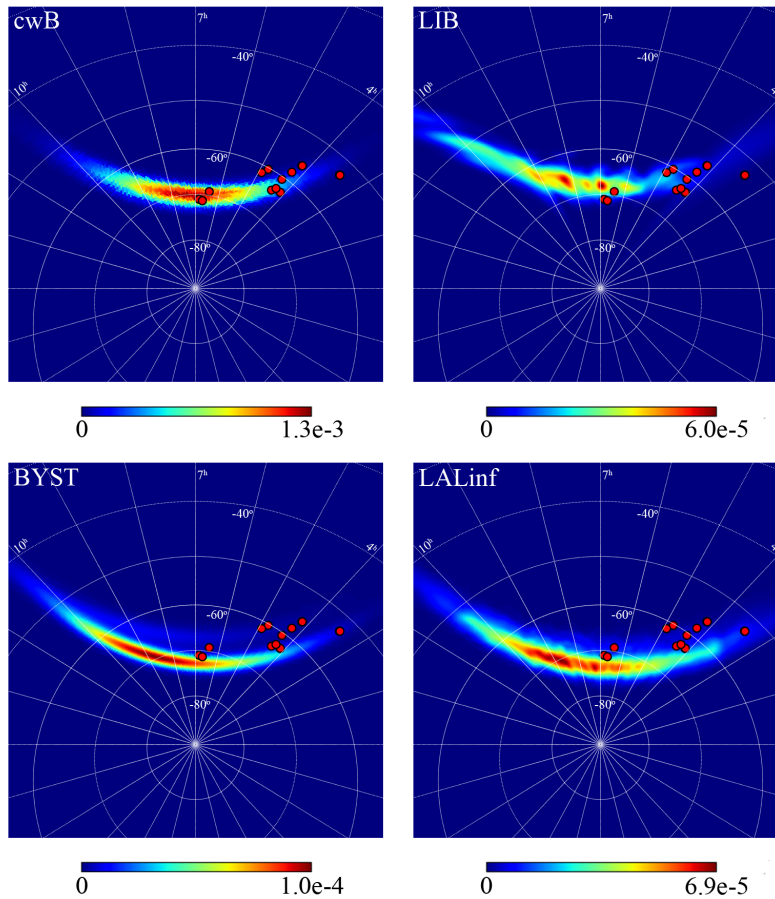


FIG. 1.— Localization probability maps for GW150914 generated by various LIGO pipelines, indicating the location of the TOROS targets (red dots).

Bayesian decision trees that uses all-sky catalogs such as USNO-B (Monet et al. 2003), 2MASS (Skrutskie et al. 2006) and *GALEX* (Martin & *GALEX* Science Team 2003).

Flux calibration was obtained by performing aperture photometry with DAOPHOT (Stetson 1987) and matching the resulting star lists against the APASS catalog (Henden et al. 2016); we found 208 stars in common

with $0.4 < B - i < 3.2$. The photometric solution was based on the r band since it exhibited the smallest color term for our unfiltered observations, yielding a zeropoint uncertainty of 0.054 mag. We used the reported photometric errors from DAOPHOT and our photometric calibration to estimate a median 5σ limiting magnitude of $r = 21.7 \pm 0.3$ mag for our fields.

3.1. Difference Imaging Analysis

We carried out two independent implementations of difference-imaging analysis (DIA) to identify transients. Most DIA routines use a kernel defined as a combination of two or more Gaussians to match and scale the point-spread-function (PSF) between two epochs (Alard & Lupton 1998), which leads to difficulties in fitting irregular shaped PSFs. Our implementations go beyond this simple approach.

Our first method (hereafter “Method I”), described in Oelkers et al. (2015), uses a Dirac δ -function kernel fit across the entire frame. We selected the epoch with the smaller PSF to act as the reference frame. Additionally 13×13 pix stamps were taken around isolated stars with photometric precision better than 0.05 mag to solve for the kernel coefficients using the least-squares method. We modeled the spatial variation in the PSF with a 9×9 pix first-order kernel (Alard 2000; Miller et al. 2008) if there were at least 20 stars to solve for the coefficients; otherwise, we adopted a constant PSF.

The second algorithm (hereafter, “Method II”) relies on an independent pixel-by-pixel fit of the convolving kernel (Bramich 2008) with a simultaneous polynomial local background fit on the grid of an image. One of the advantages of this method is that the basis functions are removed, so the user does not need to choose a kernel (which in some cases could become inappropriate). Moreover, the basis functions are constructed around the origin of the kernel coordinate system, which requires a very good alignment of the images for an optimal result. However, the strongest caveat of this method is the type of grid used to cover the image, as kernels may change abruptly from site to site, due to the fact that there is no kernel interpolation applied between image subsections. Although an overabundance of spurious subtraction artifacts (“bogus” detections) is obtained with this method, both methods appear to be very effective and have shown similar results.

3.2. Real/Bogus classification and detection of potential transients

We trained a supervised machine-learning algorithm to discriminate between bona fide astrophysical transients and “bogus” detections arising from DIA artifacts. In order to do so, we injected 100 artificial stars on each of the 21 science images, repeating the procedure 10 times to improve our statistics, and subjected the resulting 210 frames to the same DIA methods described above. The injections followed the same magnitude distribution as the point sources detected by DAOPHOT in the reference images.

We ran SExtractor (Bertin & Arnouts 1996) on the differenced image products from both methods to detect objects with a significance of $> 2\sigma$ and with > 5 connected pixels and extract their defining characteristics (such as magnitude, magnitude error, ellipticity and sharpness). We identified the objects that corresponded to known injected sources and labeled them accordingly. We used a random-forest algorithm with $5 \times$ cross validation to identify any other sources exhibiting properties similar to the injections, as potential astrophysical transients. We rejected all other remaining sources, here-after identified as “bogus”.

TABLE 2
CONFUSION MATRIX AT
 $p = 0.5$

Actual	Prediction	
	1	0
1	0.961	0.038
0	0.046	0.953

4. RESULTS

SExtractor detected ~ 10400 and ~ 34000 objects on the 210 frames processed with Methods I & II, respectively; of these, 5441 and 5824 were recovered artificial stars. We used these recovered injections to define the set of features needed to identify “real” detections and remove “bogus” candidates.

Fig. 2 shows the results of the Random Forest classification, including model accuracy vs. confidence and the Receiver Operating Curve (ROC) for the set of transients obtained through Method I (defined in §3.1). The upper panel also shows the average accuracy (upper dashed line) and the probability of obtaining the same result by chance (dashed-dotted line). The latter is computed using the P_e statistic, defined as the sum of the probabilities of the model for either predicting a “real” transient (P_r) or a “bogus” event (P_b): $P_e = P_r + P_b$. The respective probabilities are calculated as follows:

$$P_e = \left[\left(\frac{A_r}{N} \right) \left(\frac{P_r}{N} \right) + \left(\frac{A_b}{N} \right) \left(\frac{P_b}{N} \right) \right] \quad (1)$$

where A_r and A_b is the number of injections and unknowns and N is the total number of objects in the sample.

We used the ROC to calculate Youden’s statistic (Youden 1950) or informedness $J_{\max} = 0.91 \pm 0.0039$, where the quoted error represents the 95% confidence level (Powers 2011). J_{\max} gives the maximum performance of the model and is defined as the maximum distance between the ROC and the 1:1 line that represents the probability of obtaining the result by chance. The observed value of J_{\max} corresponds to a cutoff of 0.49 in terms of the confidence value. It is in good agreement with the maximum accuracy of 0.96 reached by the classifier, as seen in Fig. 2. We therefore selected a cutoff value of 0.5 for our final analysis and the resulting confusion matrix is presented in Table 2.

Following these procedures, we identified 229 and 200 objects in all the images processed by Methods I & II, respectively, as having probabilities greater than 50% of being real. As a final discrimination against spurious detections, we required an object to be detected in at least 5 of 10 realizations of a given field in order to be considered a *bona fide* astrophysical transient. None of the objects in either set passed this requirement. Further visual inspection revealed most of them to be subtraction residuals or cosmetic defects in the detector. We therefore conclude that no transients were present in the 21 fields we targeted, to a 5σ limiting magnitude of $r = 21.7$ mag. Similar results were obtained for Method II, albeit with a higher fraction of “bogus” sources, a result leading to a less balanced sample to merit further analysis.

The fact that we did not find any genuine transient in our search is not surprising given the small area surveyed

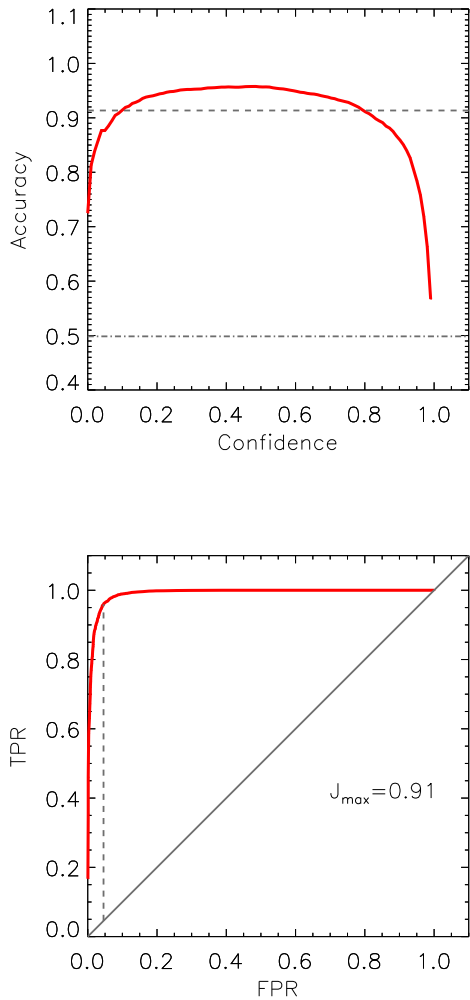


FIG. 2.— Top: Plot of model accuracy vs. confidence. Bottom: Receiver Operating Curve. See text for details.

($\sim 0.62^\circ$) and the low cadence of the observations (with only two epochs per target, separated by 73 ± 3 d). Based on our temporal sampling and photometric precision, we scaled the results of Oelkers et al. (2015, 2016) to estimate that only 1 in ~ 3030 stars in our fields would exhibit variability detectable at the 5σ level over this timescale. Given that only ~ 4200 stars were detected across all fields by DAOPHOT, we would only expect to detect ~ 1 variable star. Regarding extragalactic transients, based on supernova Ia rate for $R < 21$ mag of 10

events per square degree per year (Pain et al. 1996; Garavich et al. 2004) and a 30% fraction of SN Ia among local SNe (Guillochon et al. 2016), we estimate an 11% probability of finding such an object across all our fields. Finally, our result is consistent with the LIGO detection of a binary black hole merger, for which no optical EM counterpart is expected.

5. SUMMARY

The TOROS collaboration conducted a prompt search for the electromagnetic counterpart of the first gravitational-wave event reported by LIGO using the 1.5-m telescope of Estación Astrofísica Bosque Alegre (EABA) in Córdoba, Argentina. Our search spanned two nights, during which we targeted 21 fields containing 14 nearby ($D < 60$ Mpc) galaxies with high probabilities of hosting the event. We covered 0.62° and reached a 5σ limiting AB magnitude of $r = 21.7$. We used a combination of difference-imaging techniques and machine-learning procedures to detect and classify potential transients. No *bona fide* events were found, a result that is consistent with the low probability of detecting stellar or extragalactic variability given our temporal and areal coverage, and with the later classification of the GW event as a merger of two stellar-mass black holes.

Our host-galaxy ranking approach serves as a complementary strategy to the wide-field surveys for these transients, such as those conducted by the Dark Energy Survey (Annis et al. 2016; Soares-Santos et al. 2016), the intermediate Palomar Transient Factory (Kasliwal et al. 2016), MASTER (Lipunov et al. 2016), Pan-STARRS (Smartt et al. 2016), and the VLT Survey Telescope (E. Brocato et al, in preparation). Given the incompleteness of local galaxy catalogs, the rapid dissemination of possible counterpart candidates by the wide-field surveys would enable detailed photometric coverage to be contributed by many modest-aperture, narrow-field telescopes throughout the world. Additionally, unfiltered CCD observations may be desirable at this stage given the large uncertainties in the possible colors of these counterparts.

The TOROS collaboration acknowledges support from Ministerio de Ciencia, Tecnología e Innovación Productiva (MinCyT) and Consejo Nacional de Investigaciones Científicas y Tecnológicas (CONICET) from Argentina, grants from the National Science Foundation of the United States of America, NSF PHYS 1156600 and NSF HRD 1242090, and the government of Salta province in Argentina.

Facilities: EABA.

REFERENCES

- Abadie, J., Abbott, B. P., Abbott, R., et al. 2012, *A&A*, 541, A155
 Abbott, B. P., Abbott, R., Abbott, T. D., et al. 2016a, *Physical Review Letters*, 116, 061102
 —. 2016b, *Living Reviews in Relativity*, 19, arXiv:1304.0670
 —. 2016c, *Astrophysical Journal Supplement Series*, 225, 8
 Acernese, F., Agathos, M., Agatsuma, K., et al. 2015, *Classical and Quantum Gravity*, 32, 024001
 Alard, C. 2000, *A&AS*, 144, 363
 Alard, C., & Lupton, R. H. 1998, *ApJ*, 503, 325
 Annis, J., Soares-Santos, M., Berger, E., et al. 2016, *ApJ*, 823, L34
 Barnes, J., & Kasen, D. 2013, *ApJ*, 775, 18
 Belczynski, K., Kalogera, V., & Bulik, T. 2002, *ApJ*, 572, 407
 Benacquista, M., Belczynski, C., Berioz, M., et al. 2014, in *EAS Publications Series*, Vol. 67, *EAS Publications Series*, 357–358
 Berger, E. 2014, *ARA&A*, 52, 43
 Bertin, E., & Arnouts, S. 1996, *A&AS*, 117, 393

- Bramich, D. M. 2008, *MNRAS*, 386, L77
- Church, R. P., Levan, A. J., Davies, M. B., & Tanvir, N. 2011, *MNRAS*, 413, 2004
- Cowperthwaite, P. S., & Berger, E. 2015, *ApJ*, 814, 25
- Essick, R., Vitale, S., Katsavounidis, E., Vedovato, G., & Klimentko, S. 2015, *ApJ*, 800, 81
- Fong, W., & Berger, E. 2013, *ApJ*, 776, 18
- Garnavich, P. M., Smith, R. C., Miknaitis, G., et al. 2004, in *Bulletin of the American Astronomical Society*, Vol. 36, American Astronomical Society Meeting Abstracts, 1530
- Guillochon, J., Parrent, J., & Margutti, R. 2016, *ArXiv e-prints*, arXiv:1605.01054
- Hanna, C., Mandel, I., & Vouden, W. 2014, *ApJ*, 784, 8
- Henden, A. A., Templeton, M., Terrell, D., et al. 2016, *VizieR Online Data Catalog*, 2336
- Kasliwal, M. M., Cenko, S. B., Singer, L. P., et al. 2016, *ApJ*, 824, L24
- Klimentko, S., Vedovato, G., Drago, M., et al. 2016, *Phys. Rev. D*, 93, 042004
- Lang, D. 2009, PhD thesis, University of Toronto, Canada
- Li, L.-X., & Paczyński, B. 1998, *ApJ*, 507, L59
- LIGO Scientific Collaboration, Aasi, J., Abbott, B. P., et al. 2015, *Classical and Quantum Gravity*, 32, 074001
- Lipunov, V. M., Kornilov, V., Gorbovskoy, E., et al. 2016, *ArXiv e-prints*, arXiv:1605.01607
- Lynch, R., Vitale, S., Essick, R., Katsavounidis, E., & Robinet, F. 2015, *ArXiv e-prints*, arXiv:1511.05955
- Martin, C., & GALEX Science Team. 2003, in *Bulletin of the American Astronomical Society*, Vol. 35, American Astronomical Society Meeting Abstracts, 1363
- Metzger, B. D., & Berger, E. 2012, *ApJ*, 746, 48
- Miller, J. P., Pennypacker, C. R., & White, G. L. 2008, *PASP*, 120, 449
- Monet, D. G., Levine, S. E., Canzian, B., et al. 2003, *AJ*, 125, 984
- Nakar, E., & Piran, T. 2011, *Nature*, 478, 82
- Nuttall, L. K., & Sutton, P. J. 2010, *Phys. Rev. D*, 82, 102002
- Oelkers, R. J., Macri, L. M., Wang, L., et al. 2015, *AJ*, 149, 50
- . 2016, *ArXiv e-prints*, arXiv:1603.09699
- Pain, R., Hook, I. M., Deustua, S., et al. 1996, *ApJ*, 473, 356
- Phinney, E. S. 1991, *ApJ*, 380, L17
- Planck Collaboration, Ade, P. A. R., Aghanim, N., et al. 2015, *ArXiv e-prints*, arXiv:1502.01589
- Powers, D. M. 2011, *Journal of Machine Learning Technologies*, 2, 37
- Renzi, V., Vrech, R., Ferreiro, D., et al. 2009, *Boletín de la Asociación Argentina de Astronomía La Plata Argentina*, 52, 285
- Singer, L. 2015, *GRB Coordinates Network*, 18330
- Skrutskie, M. F., Cutri, R. M., Stiening, R., et al. 2006, *AJ*, 131, 1163
- Smartt, S. J., Chambers, K. C., Smith, K. W., et al. 2016, *ArXiv e-prints*, arXiv:1602.04156
- Soares-Santos, M., Kessler, R., Berger, E., et al. 2016, *ApJ*, 823, L33
- Stetson, P. B. 1987, *PASP*, 99, 191
- Tremblin, P., Schneider, N., Minier, V., Durand, G. A., & Urban, J. 2012, *A&A*, 548, A65
- White, D. J., Daw, E. J., & Dhillon, V. S. 2011, *Classical and Quantum Gravity*, 28, 085016
- Youden, W. J. 1950, *Cancer*, 3, 32